

GRANTS

This research was partly supported by a Grant-in-Aid for Scientific Research (21590320 to K. Tsuchida) from the Japan Society for the Promotion of Science, a Grant-in-Aid for Young Scientists (22790328 to M. Nakatani) from JSPS, a research grant (H20-018) on psychiatric and neurological diseases and mental health from the Ministry of Health, Labour and Welfare, and an Intramural Research Grant (20B-13) for Neurological and Psychiatric Disorders of National Center of Neurology and Psychiatry.

DISCLOSURES

No conflicts of interest are reported by the authors.

REFERENCES

- Akpan I, Goncalves MD, Dhir R, Yin X, Pistilli EE, Bogdanovich S, Khurana TS, Ucran J, Lachey J, Ahima RS. The effects of a soluble activin type IIB receptor on obesity and insulin sensitivity. *Int J Obes (Lond)* 33: 1265–1273, 2009.
- Amthor H, Nicholas G, McKinnell I, Kemp CF, Sharma M, Kambadur R, Patel K. Follistatin complexes Myostatin and antagonizes Myostatin-mediated inhibition of myogenesis. *Dev Biol* 270: 19–30, 2004.
- Archibald FM, Skipski VP. Determination of fatty acid content and composition in ultramicro lipid samples by gas-liquid chromatography. *J Lipid Res* 7: 442–445, 1966.
- Bligh EG, Dyer WJ. A rapid method of total lipid extraction and purification. *Can J Biochem Physiol* 37: 911–917, 1959.
- Boman IA, Klemetsdal G, Blichfeldt T, Nafstad O, Vage DI. A frameshift mutation in the coding region of the myostatin gene (MSTN) affects carcass conformation and fatness in Norwegian White Sheep (*Ovis aries*). *Anim Genet* 40: 418–422, 2009.
- Brand MD, Esteves TC. Physiological functions of the mitochondrial uncoupling proteins UCP2 and UCP3. *Cell Metab* 2: 85–93, 2005.
- Chan CB, Harper ME. Uncoupling proteins: role in insulin resistance and insulin insufficiency. *Curr Diabetes Rev* 2: 271–283, 2006.
- Clop A, Marcq F, Takeda H, Pirottin D, Tordoir X, Bibe B, Bouix J, Caiment F, Elsen JM, Eychenne F, Larzul C, Laville E, Meish F, Milenkovic D, Tobin J, Charlier C, Georges M. A mutation creating a potential illegitimate microRNA target site in the myostatin gene affects muscularity in sheep. *Nat Genet* 38: 813–818, 2006.
- Dobrzyn A, Ntambi JM. Stearoyl-CoA desaturase as a new drug target for obesity treatment. *Obes Rev* 6: 169–174, 2005.
- Feldman BJ, Streepfer RS, Farese RV Jr, Yamamoto KR. Myostatin modulates adipogenesis to generate adipocytes with favorable metabolic effects. *Proc Natl Acad Sci USA* 103: 15675–15680, 2006.
- Gamer LW, Cox KA, Small C, Rosen V. Gdf11 is a negative regulator of chondrogenesis and myogenesis in the developing chick limb. *Dev Biol* 229: 407–420, 2001.
- Gilson HM, Schakman OR, Kalista S, Lause P, Tsuchida K, Thissen JP. Follistatin induces muscle hypertrophy through satellite cell proliferation and inhibition of both myostatin and activin. *Am J Physiol Endocrinol Metab* 297: E157–E164, 2009.
- Guo T, Jou W, Chanturiya T, Portas J, Gavrilova O, McPherron AC. Myostatin inhibition in muscle, but not adipose tissue, decreases fat mass and improves insulin sensitivity. *PLoS One* 4: e4937, 2009.
- Hamrick MW, Pennington C, Webb CN, Isaacs CM. Resistance to body fat gain in “double-muscled” mice fed a high-fat diet. *Int J Obes (Lond)* 30: 868–870, 2006.
- Hill JJ, Davies MV, Pearson AA, Wang JH, Hewick RM, Wolfman NM, Qiu Y. The myostatin propeptide and the follistatin-related gene are inhibitory binding proteins of myostatin in normal serum. *J Biol Chem* 277: 40735–40741, 2002.
- Hock MB, Kralli A. Transcriptional control of mitochondrial biogenesis and function. *Annu Rev Physiol* 71: 177–203, 2009.
- Ishigaki Y, Katagiri H, Yamada T, Oghihara T, Imai J, Uno K, Hasegawa Y, Gao J, Ishihara H, Shimosegawa T, Sakoda H, Asano T, Oka Y. Dissipating excess energy stored in the liver is a potential treatment strategy for diabetes associated with obesity. *Diabetes* 54: 322–332, 2005.
- Krauss S, Zhang CY, Lowell BB. The mitochondrial uncoupling-protein homologues. *Nat Rev Mol Cell Biol* 6: 248–261, 2005.
- Lee SJ. Regulation of muscle mass by myostatin. *Annu Rev Cell Dev Biol* 20: 61–86, 2004.
- Li L, Shen JJ, Bournat JC, Huang L, Chattopadhyay A, Li Z, Shaw C, Graham BH, Brown CW. Activin signaling: effects on body composition and mitochondrial energy metabolism. *Endocrinology* 150: 3521–3529, 2010.
- McPherron AC, Huynh TV, Lee SJ. Redundancy of myostatin and growth/differentiation factor 11 function. *BMC Dev Biol* 9: 24, 2009.
- McPherron AC, Lawler AM, Lee SJ. Regulation of skeletal muscle mass in mice by a new TGF-beta superfamily member. *Nature* 387: 83–90, 1997.
- McPherron AC, Lee SJ. Double muscling in cattle due to mutations in the myostatin gene. *Proc Natl Acad Sci USA* 94: 12457–12461, 1997.
- McPherron AC, Lee SJ. Suppression of body fat accumulation in myostatin-deficient mice. *J Clin Invest* 109: 595–601, 2002.
- Miyazaki M, Flowers MT, Sampath H, Chu K, Otzelberger C, Liu X, Ntambi JM. Hepatic stearoyl-CoA desaturase-1 deficiency protects mice from carbohydrate-induced adiposity and hepatic steatosis. *Cell Metab* 6: 484–496, 2007.
- Mosher DS, Quignon P, Bustamante CD, Sutter NB, Mellersh CS, Parker HG, Ostrander EA. A mutation in the myostatin gene increases muscle mass and enhances racing performance in heterozygote dogs. *PLoS Genet* 3: e79, 2007.
- Nakatani M, Takehara Y, Sugino H, Matsumoto M, Hashimoto O, Hasegawa Y, Murakami T, Uezumi A, Takeda S, Noji S, Sunada Y, Tsuchida K. Transgenic expression of a myostatin inhibitor derived from follistatin increases skeletal muscle mass and ameliorates dystrophic pathology in mdx mice. *FASEB J* 22: 477–487, 2008.
- Ntambi JM, Miyazaki M. Recent insights into stearoyl-CoA desaturase-1. *Curr Opin Lipidol* 14: 255–261, 2003.
- Ohsawa Y, Hagiwara H, Nakatani M, Yasue A, Moriyama K, Murakami T, Tsuchida Noji S K, Sunada Y. Muscular atrophy of caveolin-3-deficient mice is rescued by myostatin inhibition. *J Clin Invest* 116: 2924–2934, 2006.
- Pangas SA, Jorgez CJ, Tran M, Agno J, Li X, Brown CW, Kumar TR, Matzuk MM. Intraovarian activins are required for female fertility. *Mol Endocrinol* 21: 2458–2471, 2007.
- Saito S, Sugino K, Yamanouchi K, Kogawa K, Titani K, Shiota K, Takahashi M, Sugino H. Characterization of antisera directed against follistatin/activin-binding protein peptides. *Endocrinol Jpn* 38: 377–382, 1991.
- Schuelke M, Wagner KR, Stolz LE, Hubner C, Riebel T, Komen W, Braun T, Tobin JF, Lee SJ. Myostatin mutation associated with gross muscle hypertrophy in a child. *N Engl J Med* 350: 2682–2688, 2004.
- Shelton GD, Engvall E. Gross muscle hypertrophy in whippet dogs is caused by a mutation in the myostatin gene. *Neuromuscul Disord* 17: 721–722, 2007.
- Siriatt V, Salerno MS, Berry C, Nicholas G, Bower R, Kambadur R, Sharma M. Antagonism of myostatin enhances muscle regeneration during sarcopenia. *Mol Ther* 15: 1463–1470, 2007.
- Stolz LE, Li D, Qadri A, Jalenak M, Klaman LD, Tobin JF. Administration of myostatin does not alter fat mass in adult mice. *Diabetes Obes Metab* 10: 135–142, 2008.
- Sugino K, Kurosawa N, Nakamura T, Takio K, Shimasaki S, Ling N, Titani K, Sugino H. Molecular heterogeneity of follistatin, an activin-binding protein. Higher affinity of the carboxyl-terminal truncated forms for heparan sulfate proteoglycans on the ovarian granulosa cell. *J Biol Chem* 268: 15579–15587, 1993.
- Tsuchida K. Activins, myostatin and related TGF-beta family members as novel therapeutic targets for endocrine, metabolic and immune disorders. *Curr Drug Targets Immune Endocr Metabol Disord* 4: 157–166, 2004.
- Tsuchida K. Targeting myostatin for therapies against muscle-wasting disorders. *Curr Opin Drug Discov Devel* 11: 487–494, 2008.
- Whittemore LA, Song K, Li X, Aghajanian J, Davies M, Girgenrath S, Hill JJ, Jalenak M, Kelley P, Knight A, Maylor R, O'Hara D, Pearson A, Quazi A, Ryerson S, Tan XY, Tomkinson KN, Veldman GM, Widom A, Wright JF, Wudyka S, Zhao L, Wolfman NM. Inhibition of myostatin in adult mice increases skeletal muscle mass and strength. *Biochem Biophys Res Commun* 300: 965–971, 2003.
- Wolfman NM, McPherron AC, Pappano WN, Davies MV, Song K, Tomkinson KN, Wright JF, Zhao L, Sebald SM, Greenspan DS, Lee SJ. Activation of latent myostatin by the BMP-1/tolloid family of metalloproteinases. *Proc Natl Acad Sci USA* 100: 15842–15846, 2003.
- Yang J, Zhao B. Postnatal expression of myostatin propeptide cDNA maintained high muscle growth and normal adipose tissue mass in transgenic mice fed a high-fat diet. *Mol Reprod Dev* 73: 462–469, 2006.
- Zhao B, Wall RJ, Yang J. Transgenic expression of myostatin propeptide prevents diet-induced obesity and insulin resistance. *Biochem Biophys Res Commun* 337: 248–255, 2005.

Original Article

Delivery of small interfering RNA with a synthetic collagen poly(Pro-Hyp-Gly) for gene silencing *in vitro* and *in vivo*Taro Adachi,¹ Emi Kawakami,² Naozumi Ishimaru,³ Takahiro Ochiya,⁴ Yoshio Hayashi,³ Hideyo Ohuchi,¹ Masao Tanihara,⁵ Eiji Tanaka² and Sumihare Noji^{1*}

¹Department of Life Systems, Institute of Technology and Science, The University of Tokushima Graduate School, 2-1 Minami-Jyosanjima; ²Department of Orthodontics and Dentofacial Orthopedics, Institute of Health Bioscience, The University of Tokushima Graduate School, 3-18-15 Kuramotocho; ³Department of Oral Molecular Pathology, Institute of Health Biosciences, University of Tokushima Graduate School, Kuramotocho, Tokushima 770-8504; ⁴National Cancer Center Research Institute, Chuo-ku, Tokyo 104-0045; ⁵Graduate School of Materials Science, Nara Institute of Science and Technology, Ikoma, Nara 630-0192, Japan

Silencing gene expression by small interfering RNAs (siRNAs) has become a powerful tool for the genetic analysis of many animals. However, the rapid degradation of siRNA and the limited duration of its action *in vivo* have called for an efficient delivery technology. Here, we describe that siRNA complexed with a synthetic collagen poly(Pro-Hyp-Gly) (SYCOL) is resistant to nucleases and is efficiently transferred into cells *in vitro* and *in vivo*, thereby allowing long-term gene silencing *in vivo*. We found that the SYCOL-mediated local application of siRNA targeting *myostatin*, coding a negative regulator of skeletal muscle growth, in mouse skeletal muscles, caused a marked increase in the muscle mass within a few weeks after application. Furthermore, *in vivo* administration of an anti-luciferase siRNA/SYCOL complex partially reduced luciferase expression in xenografted tumors *in vivo*. These results indicate a SYCOL-based non-viral delivery method could be a reliable simple approach to knockdown gene expression by RNAi *in vivo* as well as *in vitro*.

Key words: delivery, myostatin, RNAi, siRNA, synthetic collagen.

Introduction

Induction of RNA interference (RNAi) by small interfering RNA (siRNA) is a useful method for knocking down molecular targets specifically (Tiemann & Rossi 2009). However, there exists a delivery problem: The siRNA alone can not be transported across cell membranes to the cytosol, due to its large molecular weight (~13 kDa) and strong anionic charge of the siRNA phosphodiester backbone (~40 negative phosphate charges) (Behlke 2006). Consequently, carrier development for siRNA delivery has been one of the most important problems to solve before siRNA can achieve widespread basic and clinical use. Multiple nonviral

delivery systems have been introduced so far in order to deliver siRNA efficiently including chemical modification of siRNA, cationic polymers, cationic lipids, cell-penetrating peptide, and targeted delivery (for review, see (Kim & Kim 2009; Kim *et al.* 2009)). Several promising carriers with low toxicity and increased specificity for target cells or tissues have emerged for siRNA-based experiments (Kim *et al.* 2009).

One of the promising carriers for effective gene silencing *in vitro* and *in vivo* is Atelocollagen (ATCOL) (Minakuchi *et al.* 2004), which is a highly purified pepsin-treated type I collagen from calf dermis. ATCOL obtained by pepsin treatment is low in immunogenicity because it is free from telopeptides (Stenzel *et al.* 1974), and it has been used clinically for a wide range of purposes, including wound-healing, vessel prosthesis and also as a bone cartilage substitute and hemostatic agent (Ochiya *et al.* 2001). We previously showed that when siRNA targeting *myostatin*, coding a negative regulator of skeletal muscle growth, was introduced locally or systemically into mouse skeletal

*Author to whom all correspondence should be addressed.

Email: noji@bio.tokushima-u.ac.jp

Received 3 April 2010; revised 13 June 2010;

accepted 25 June 2010.

© 2010 The Authors

Journal compilation © 2010 Japanese Society of Developmental Biologists

muscles with ATCOL, the muscle mass markedly increased within a few weeks after application (Kinouchi *et al.* 2008). However, delivery mechanisms of siRNA by ATCOL in cells have not been elucidated yet.

In the present study, to find collagen structures essential for siRNA delivery, we examined whether a simple synthetic collagen (SYCOL) functions similarly as ATCOL. As a simple collagen-model peptide, we used a synthesized collagen poly(Pro-Hyp-Gly) which forms a stable triple-helical structure (Kishimoto *et al.* 2005), because Pro-Hyp-Gly is a characteristic amino acid sequence found in fibrous collagens. We suspended siRNA in a solution of poly(Pro-Hyp-Gly) which is sterilized by an electron beam and observed its effect on expression of target genes *in vitro* and *in vivo*. We found that the siRNA/SYCOL complex solution has a gene silencing activity in culture cells, mouse muscles, and xenografted tumors. Thus, we concluded that even a simple synthetic collagen can deliver siRNA into cells *in vivo* and *in vitro*.

Materials and methods

Collagens

In vivo siRNA transfection kit of AteloGene for systemic use containing Atelocollagen (ATCOL) (concentration 0.1%) or for local use (ATCOL concentration 1%) was purchased from KOKEN and used according to the manufacturer's instructions. We obtained a synthetic collagen poly(Pro-Hyp-Gly) (SYCOL), molecular weights greater than 10^5) made by polycondensation of Pro-Hyp-Gly as a gift by Chisso, which was sterilized by irradiation of an electron beam (40KG) for 2 min (Sanshodoh).

Preparation of siRNA

Synthetic 21-nt RNAs were purchased from KOKEN. The sequences of the mouse growth differentiation factor (DGF)-8 (myostatin) siRNA are 5'-AAGAUGACG-AUUAUCACGCUA-3' and 3'-UUCUACUGCAAUAG-UGCGAU-5'.

The control sequences of scramble siRNA are 5'-AUCGAAUAACCGUAACGUUGA-3' and 3'-UAGCUUAU-UGGCAUUGCAACU-5'. The control siRNA duplex and Firefly luciferase GL3 siRNA duplex were purchased from Nippon gene.

Formation of siRNA/synthetic collagen complex

The siRNAs and the collagen complexes were prepared as follows. Equal volumes of collagen (in

phosphate buffered saline (PBS) at pH 7.4) and siRNAs solution were combined and mixed by vigorous pipetting. The final concentration of the collagen was 0.03%. The complex was then kept at 4°C for 16 h before use.

Stability tests of siRNA/collagen complex

An aliquot of 0.9 µg of siRNAs (luciferase GL3 duplex) complexed with lipofectamin 2000 (Invitrogen), ATCOL (concentration 0.5%), ATCOL (0.05%) or SYCOL (0.03%) was incubated in the presence of 0.1 µg/µL RNase A (Nippon gene) for 0, 5, 15, 30, 45 and 60 min at 37°C. The siRNAs were extracted from the reaction solution with phenol and phenol/chloroform/isoamyl alcohol (25:24:1). Then, the siRNAs were precipitated with ethanol and polyacrylamide gel electrophoresed (25%) and visualized by ethidium bromide staining.

Cell lines

B16-F10-luc-G5 melanoma cells continuously expressing luciferase (Xenogen) were maintained in Dulbecco's Modified Eagle Medium (DMEM) with 10% heat-inactivated fetal bovine serum (FBS) and Zeocin (0.2 mg/mL) at 37°C in a humidified atmosphere of 5% CO₂.

Synthetic collagen-mediated siRNA transfer

The siRNA/SYCOL (0.03%) complexes were prefixed to a 24 well plate (10–173 pmol siRNA/50 µL/well) according to the method described previously (Minakuchi *et al.* 2004). The cultured cells were plated into the complex-prefixed 24 well plate at 3.5×10^4 B16-F10-luc-G5 melanoma cells/well and the effects of siRNA transfer were then measured by a luciferase assay. The cationic liposome-mediated transfer of siRNA was performed as described by the manufacturer (Invitrogen).

Luciferase assays

For luciferase-based reporter gene assays, B16-F10-luc-G5 cells were used. The cells were collected by trypsinization and plated in the 24-well dishes for siRNA transfection. SYCOL- or ATCOL-mediated or conventional transfection of siRNAs into cells was performed in accordance with the manufacturer's instructions. Cells were lysed ($n = 3$) on day 2 and analyzed for luciferase activity (Microplate reader Model 680; Bio-Rad).

Effects of SYCOL-mediated local transfer of siRNA against myostatin in muscles

siRNAs against *Myostatin* (final concentration, 10 μ M) were mixed with SYCOL (final concentration for local administration, 0.03%) or ATCOL (0.05%) according to the manufacturer's instructions. After anesthesia of mice (20-week-old male C57BL/6) by Nembutal (25 mg/kg, i.p.), the myostatin siRNA/SYCOL (myostatin-siRNA/SYCOL) complex was injected into the masseter on the left side. As a control, scrambled siRNA/SYCOL complex was injected into the contralateral (right) muscles. After 2 weeks, the muscles on both sides were isolated and processed for analysis.

Real-time quantitative RT-PCR

Total RNA was extracted from the masseter muscle, and reverse transcribed. Transcript levels of *myostatin* were measured using DNA Engine OPTICON system (Bio-Rad) with SYBR Premix Ex Tag (Takara Shuzo). The specific primers used were as follows; 5'-CAG CCT GAA TCC AAC TTA GG-3' (Forward primer, region 758), 3'-TCG CAG TCA AGC CCA AAG TC-5' (Reverse Primer, region 905).

Monitoring luciferase inhibition in vivo with bioluminescent imaging

B16-F10-luc-G5 cells were subcutaneously injected (1×10^6 cells/100 μ L) into athymic nude mice inferior ophthalmic vein of right eye. Seven days later, 200 μ L of each solution containing luciferase GL3 siRNA/ATCOL (0.05%), luciferase GL3 siRNA/SYCOL (0.03%), SYCOL alone, or luciferase GL3 siRNA alone was injected into the mouse inferior ophthalmic vein of the left eye. For *in vivo* imaging, D-luciferin (150 mg/kg; WAKO) was injected into the mouse inferior ophthalmic vein of the right eye. Fifteen minutes later, photons from animal whole bodies were counted by using the IVIS imaging system (Xenogen) according to the manufacturer's instructions. Data were analyzed by using LIVINGIMAGE 2.50 software (Xenogen). A successful injection was indicated by day 0 images that showed a systemic bioluminescence distributed throughout the animal, and only those mice evidencing a satisfactory injection were used in the continued experiment. The siRNA/SYCOL and siRNA/ATCOL effects were monitored after 3 days *in vivo* by bioluminescent imaging. Tumor growth was not affected by these treatments.

For preparing the siRNA/SYCOL complex, an equal volume of SYCOL (0.06% in distilled water at pH 5.6) and siRNA solution was combined and mixed by rotating for 20 min at 4°C. For preparing the siRNA/ATCOL

complex, equal volumes of ATCOL (0.1% in siRNA buffer by KOKEN) and siRNA solution were combined and mixed by rotating for 20 min at 4°C. The siRNAs or their complexes were directly injected into the mouse inferior ophthalmic vein of the left eye. The final concentrations of SYCOL and ATCOL were 0.03% and 0.05%, respectively. The siRNA concentration used in the liposome experiments was 4 nmol/mouse equivalent to that used in the SYCOL or ATCOL experiments. *In vivo* bioimaging was conducted on a cryogenically cooled IVIS system (Xenogen) using LivingImage acquisition and analysis software (Vooijs *et al.* 2002).

Statistical analysis

The results are given as means \pm standard error (SE). Statistical analysis was conducted using the analysis of variance with the Bonferroni correction for multiple comparisons. A *P*-value of 0.05 or less was considered to indicate a significant difference.

Results

In vitro delivery of siRNA with a synthetic collagen poly(Pro-Hyp-Gly)

In the case of Atelocollagen (ATCOL), it has been reported that the siRNA (luciferase GL3 duplex)/ATCOL complex shows resistance to degradation of siRNA in the presence of RNase A (Minakuchi *et al.* 2004). To examine whether a synthetic collagen poly(Pro-Hyp-Gly) (SYCOL) can block degradation of siRNA (luciferase GL3 duplex) from the RNase, siRNA/SYCOL complex solution was incubated in the presence of the RNase (0.1 μ g/ μ L) for 0, 5, 15, 30, 45 and 60 min at 37°C. For comparison, the same experiment was carried out with naked siRNA, siRNA/liposome complex and siRNA/ATCOL complex. Results obtained by polyacrylamide gel electrophoresis (PAGE) are shown in Fig. 1, where the siRNA/SYCOL (0.03%) complex showed partial resistance to degradation of siRNA by the RNase, similarly to the siRNA/ATCOL (0.05%) complex, although the SYCOL complex (0.03%) was less resistant than the siRNA/ATCOL (a high concentration 0.5%) and the liposome complex. We attempted to perform the same experiments in higher concentrations of SYCOL. However, since heavy precipitation in a stock solution of SYCOL was observed in a higher concentration than 0.06%, we could not estimate the resistance in higher concentration than 0.03%.

Next, we compared the efficiency of the SYCOL-mediated transfer activity with that of the ATCOL-mediated one. To examine whether SYCOL has an activity

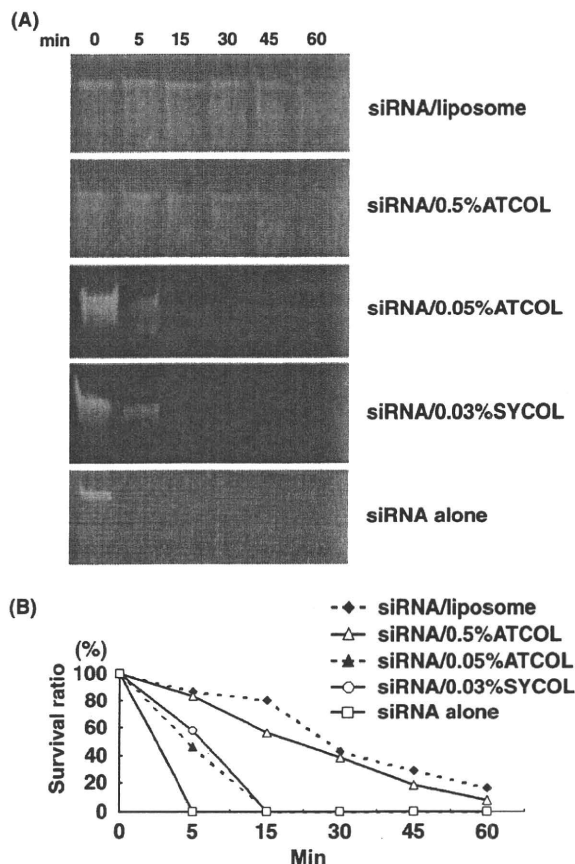


Fig. 1. A synthetic collagen poly(Pro-Hyp-Gly) (SYCOL) protects degradation of small interfering RNA (siRNA) (luciferase GL3 duplex) by RNase A. (A) siRNA (luciferase GL3 duplex)/liposome, siRNA/Atelocollagen (ATCOL) (0.5%), siRNA/ATCOL (0.05%), siRNA/SYCOL (0.03%) complexes or naked siRNA were incubated in the presence of RNase A for 0, 5, 15, 30, 45 and 60 min at 37°C and then polyacrylamide gel electrophoresed. Ethidium bromide staining revealed the presence of siRNA. (B) siRNA survival ratio (0 min, 5 min, 15 min, 30 min, 45 min or 60 min/0 min of fluorescence ratio) of RNA fragment fluorescence emitted from electrophoretic gels. Software of ImageJ (NIH, USA) was used for measurement of fluorescence intensity.

of siRNA delivery into cells, we used a luciferase reporter gene system in B16-F10-luc-G5 melanoma cells, which continuously expresses luciferase (*luc*) as a well-characterized target of siRNA. In this culture system, the siRNA (luciferase GL3 duplex)/SYCOL complex was pre-coated on a micro-well plate on which the cells were then seeded (Minakuchi *et al.* 2004). Using a *luc* assay, photon emission was detected as photon counts by a luminometer. The photon counts decrease when the cells were treated with the siRNA against *luc* complexed with the SYCOL as well as with ATCOL or

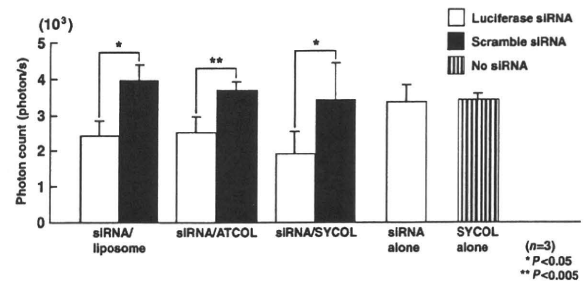


Fig. 2. A synthetic collagen poly(Pro-Hyp-Gly) (SYCOL) can transfer siRNA into cells. The luciferase siRNA duplexes were transfected into the B16-F10-luc-G5 melanoma cells to measure inhibitory effects on luciferase production of B16-F10-luc-G5 melanoma cells. Luciferase activity was measured at day 2 after transfection of siRNA/liposome, siRNA/ATCOL, siRNA/SYCOL complexes, naked siRNA or SYCOL (0.03%) solutions. White bar, luciferase siRNA; Black bar, scramble siRNA; Striped pattern bar, no siRNA.

with a liposome (Fig. 2), while no significant difference was observed in the presence of either siRNA (luciferase GL3 duplex) against *luc* alone or SYCOL alone (Fig. 2). These data indicated that the siRNA/SYCOL complex was incorporated into the cells and the siRNA can knockdown the *luc* expression as efficiently as in the presence of ATCOL or the conventional liposome. Taken together, these data showed that SYCOL can protect siRNA against RNase A and that the siRNA/SYCOL complex was able to exhibit a gene silencing effect *in vitro* as efficiently as the siRNA/ATCOL complex.

Effects of SYCOL-mediated local transfer of siRNA against myostatin in muscles

As one of the practical platforms for siRNA delivery, we previously adopted an ATCOL-mediated siRNA delivery system to apply myostatin-targeting siRNA into muscles and demonstrated that local or systemic applications of siRNA against myostatin complexed with ATCOL markedly stimulated muscle growth *in vivo* within a few weeks (Kinouchi *et al.* 2008). In order to compare efficiency of the local transfer of siRNA into muscles between SYCOL and ATCOL complexes, we performed the same experiments with SYCOL instead of using ATCOL, as reported previously (Kinouchi *et al.* 2008). We prepared the nano-particle complex containing the siRNA against *myostatin* (10 μ M) and SYCOL. Then, we injected the myostatin-siRNA/SYCOL complex into the masseter muscle of 20-week-old C57BL/6 mice. As a control, we injected scrambled siRNAs/SYCOL complex in the contralateral muscle. Two weeks after injection, we

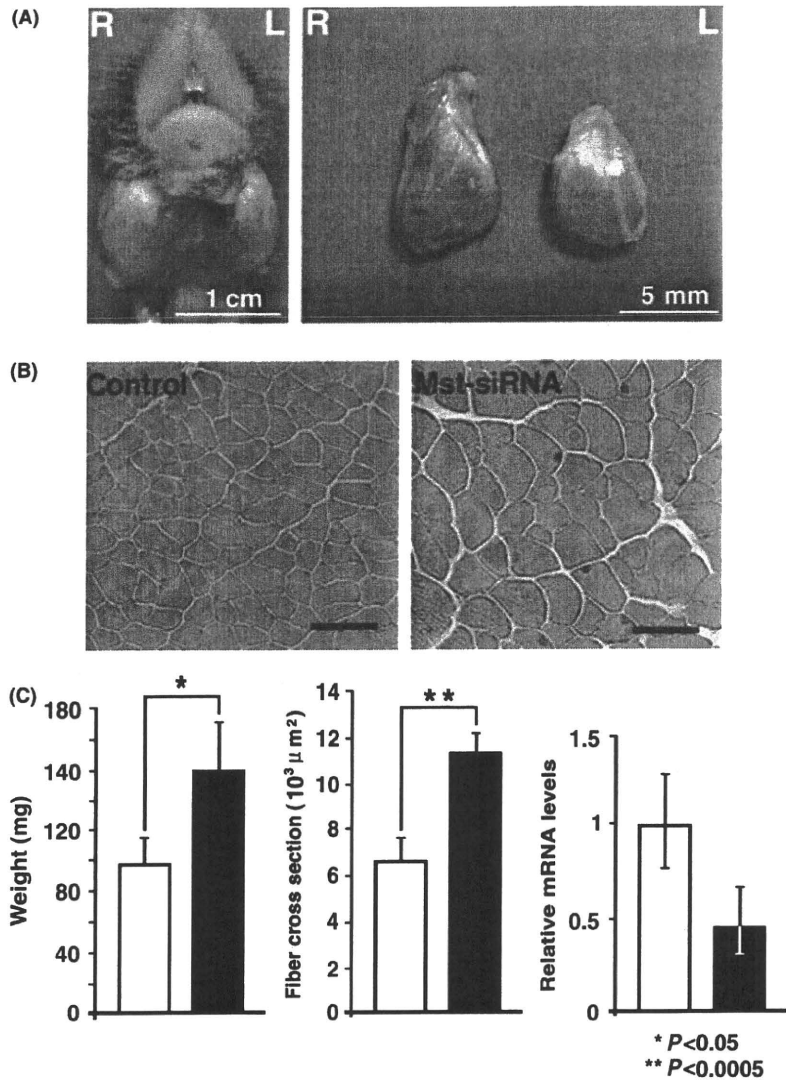


Fig. 3. Local treatment of myostatin-siRNA/synthetic collagen poly(Pro-Hyp-Gly) (SYCOL) makes the masseter muscle large in mice. Myostatin-siRNA/SYCOL treatment improves myofibril size in C57BL/6 mice. (A) Photographs of the muscles. The masseter muscles injected intramuscularly with the myostatin-siRNA/SYCOL complex show a marked increased muscle mass in 20-week-old C57BL/6 mice. (B) Hematoxylin and eosin staining of the control and myostatin-siRNA/SYCOL-treated masseter muscles. Muscles were cut to make frozen sections (5 μm thickness) at the mid-belly of the muscle and stained. Scale bar, 50 μm . (C) Average values of weights (left) and myofibril sizes (center), and the ratio of the amount of myostatin mRNA (right) for the masseter muscles. White bar, control muscles; Black bar, myostatin-siRNA/SYCOL-treated muscles.

observed gross morphology of the muscles and dissected the muscle tissues. After injection of the myostatin-siRNA/SYCOL complex, the masseter muscle (on the left side) was enlarged, while no significant change was observed on the contralateral side (Fig. 3A). Histological analysis showed that the myofibril sizes of the masseter muscles treated with the myostatin-siRNA/SYCOL complex were larger than those of the control (Fig. 3B). We also measured the muscle weight, finding that the myostatin-siRNA/SYCOL-treated muscles weighed significantly more than those on the control side (Fig. 3C, left). Examining the sizes of 200 myofibers per each group, the population of myofibril sizes indicated a shift from smaller to larger fibers in the myostatin-siRNA/SYCOL-treated muscles. The average myofibril size of the muscle treated with myostatin-siRNA/SYCOL gained approximately 1.8

times more than that of control (Fig. 3C, center), showing muscle hypertrophy. To confirm that siRNA decreased the amount of myostatin mRNA in the masseter muscle, we performed quantitative PCR (q-PCR) (Fig. 3C, right). We estimated the ratio of the amount of myostatin mRNA in the siRNA-treated muscle compared with the contralateral muscle ($n = 4$). The average ratio in the treated muscle was lowered to 0.48 ± 0.11 (in triplicate, \pm standard error), indicating that RNAi had occurred. No obvious morphological change was observed in other tissues than the treated masseter muscle. In the meantime, we did not observe any general sign of ill health and deaths during the experimental period, indicating that the siRNA complex gives no obvious adverse effects. The increase of the myostatin-siRNA/SYCOL-treated muscle mass indicated that the SYCOL system can be

used to induce a target-gene specific RNAi *in vivo* as well as the ATCOL system (Kinouchi *et al.* 2008).

Effects of intravenous administration of the siRNA/SYCOL complex in mice

To examine whether SYCOL-mediated siRNA transfer is valid for systemic gene silencing, we used mice bearing a Luc-producing melanoma described previously (Minakuchi *et al.* 2004). We carried out non-invasive *in vivo* bioluminescence imaging analysis to measure luminescence intensity (photon/s) in the tumor of mice injected with the siRNA alone, the siRNA/SYCOL complex, or siRNA/ATCOL complex (Fig. 4A). The luminescence in the tumor was observed in the head (injected site) and the abdomen at 0 day. After injection of siRNA alone or SYCOL alone, the luminescence became intense in both head and abdomen at 3 days after injection. In contrast, mice administered with the siRNA/ATCOL complex showed a relatively low intensity of the luminescence at 3 days after injection as observed by Minakuchi *et al.* (2004). In the case of the siRNA/SYCOL complex, the luminescence intensity increases in the abdomen (Fig. 4A,B), but decreases in the head region, showing sustained inhibition of luciferase expression in the head region (Fig. 4A,C). These results suggested that this SYCOL-mediated *in vivo* transfer of siRNA could be valid locally in tissues around an injected region.

Discussion

Knockdown of gene expression by RNAi becomes a powerful tool for the genetic analysis both *in vitro* and *in vivo*, while how to deliver siRNAs to the target cells and tissues has been a major challenge for RNAi based researches (Tiemann & Rossi 2009). In order to develop effective non-vector-based siRNA delivery systems for the future of siRNA-based research and therapies, we have used an ATCOL-mediated siRNA transfer systems *in vitro* and *in vivo*, because ATCOL allowed increased cellular uptake, nuclease resistance and prolonged release of siRNAs (Minakuchi *et al.* 2004). However, so far we have not known mechanisms underlying the ATCOL-mediated transfer of siRNA. In order to elucidate the mechanisms, we selected a simple synthetic collagen and examined whether it has transfer ability of siRNA into cells. Tanihara and his group developed synthetic collagen fibers poly(Pro-Hyp-Gly) (SYCOL) consisting of the Pro-Hyp-Gly sequence by direct polycondensation of Pro-Hyp-Gly tripeptides (Kishimoto *et al.* 2005). SYCOL is a polypeptide, has molecular weights greater than 10^5 and forms triple-helical, but is thermally stable up to

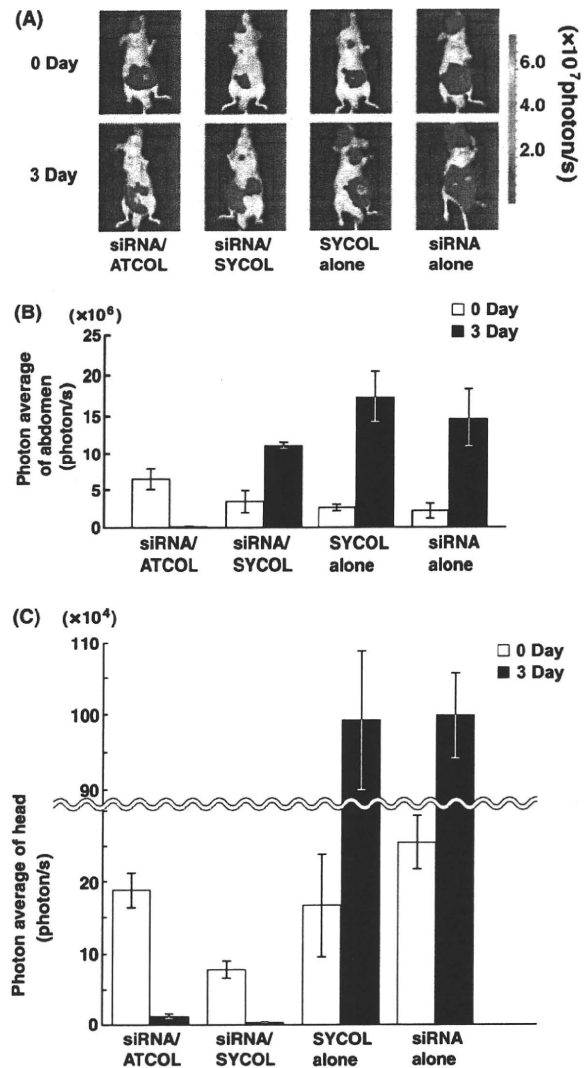


Fig. 4. Monitoring luciferase inhibition *in vivo* with bioluminescent imaging. (A) Representative images of nude mice at 3 days after tumor injection into the left ventricle of the eye with 1×10^6 B16-F10-luc-G5 cells suspended in 100 μ L of sterile phosphate-buffered saline (PBS). Each animal was given i.v. with 200 μ L of 25 μ g of GL3 siRNA/ATCOL complex, GL3 siRNA/SYCOL complex, SYCOL (0.03%) solution or luciferase GL3 siRNA. (B) Photon averages of bioluminescence emitted from the abdominal region. (C) Photon averages from the head region. White bar, photon averages at 0 day; Black bar, photon averages 3 days.

80°C and it contains no pathogens. In the present study, when we used SYCOL, a poly(Pro-Hyp-Gly) sterilized with electron-beam irradiation, instead of ATCOL, we observed significant gene-silencing effects with siRNA. Although at first we considered that only natural collagens have the ability of gene transfer, we demonstrated here that SYCOL has an activity of

silencing gene expression with siRNA. We speculate a structure of the siRNA/SYCOL complex in a buffer as follows. When SYCOLs are mixed with siRNA molecules, their terminal cationic groups may spontaneously make complex with siRNA by electrostatic interaction and form a protective outer layer that shields siRNA core, giving rise to the steric stabilization of the polyplex structure against undesirable interactions with impertinent surroundings. Since a desirable polymer structure for *in vivo* delivery purposes is a sterically stabilized but neutral, not positively charged nanoparticle (Gary *et al.* 2007), the siRNA/SYCOL complex may be a desirable one.

We also speculate a mechanism underlying cellular uptake of the siRNA/SYCOL complex as follows. Since it is known that degradation of collagen occurs primarily through a phagocytic pathway, which is required for the physiological remodeling of connective tissues during growth and development (Lee *et al.* 2007), cells may incorporate the siRNA/SYCOL complex into the cytosol probably by endocytosis.

In the case of intravenous administration of the siRNA/SYCOL complex in mice, unexpectedly we observed the silencing effect only in the head region, but not in the abdominal region. This may indicate that SYCOL itself may be somehow changed or decomposed more rapidly in blood than ATCOL and then siRNA may be released in blood. If this is the case, due to low stability of SYCOL in the blood, this RNAi is not systemic and may be induced around injected local area (in the head region, but not in the abdominal region in the present experiment).

One technical problem associated with siRNA transfer *in vivo* is the targeting of siRNA delivery to a specific tissue. For this purpose, the present SYCOL-based transfer method has great potential for site-specific transportation of target siRNAs either by way of local injection or intravenous administration. Furthermore, since SYCOL is easily modified so as to be incorporated in specific cells or tissues, for instance, to facilitate uptake by targeting cells, SYCOL could be modified chemically by conjugating with cell-targeting antibodies or ligands (Kim & Kim 2009), we may find some structures of SYCOL that are more suitable for increasing efficiency of siRNA-delivery *in vivo*.

In conclusion, we demonstrated that the siRNA/SYCOL complex is very useful to obtain gene-silencing effects. Since we can design structures of synthetic collagens, we may screen various synthetic collagens to achieve maximal function of siRNA-based gene silencing *in vivo*. Thus, a SYCOL-based siRNA transfer

system represents an attractive method for local administration of siRNA and has potential for delivery of siRNA into specific cells or tissues and thus probably for clinical applications of RNAi.

Acknowledgments

The authors thank Kawasaki Medical School for technical and financial supports. This work was supported partially by a Research Grant 20B-13 for Nervous and Mental Disorders and a Research Grant for Research on Psychiatric and Neurological Diseases and Mental Health from the Ministry of Health, Labour and Welfare.

References

- Behlke, M. A. 2006. Progress towards *in vivo* use of siRNAs. *Mol Ther.* **13**, 644–670.
- Gary, D. J., Puri, N. & Won, Y. Y. 2007. Polymer-based siRNA delivery: perspectives on the fundamental and phenomenological distinctions from polymer-based DNA delivery. *J. Control Release* **121**, 64–73.
- Kim, S.-S., Garg, H., Joshi, A. & Manjunath, N. 2009. Strategies for targeted nonviral delivery of siRNAs *in vivo*. *Trends Mol. Med.* **15**, 491–500.
- Kim, W. & Kim, S. 2009. Efficient siRNA Delivery with Non-viral Polymeric Vehicles. *Pharm. Res.* **26**, 657–666.
- Kinouchi, N., Ohsawa, Y., Ishimaru, N., Ohuchi, H., Sunada, Y., Hayashi, Y., Tanimoto, Y., Moriyama, K. & Noji, S. 2008. Atelocollagen-mediated local and systemic applications of myostatin-targeting siRNA increase skeletal muscle mass. *Gene Ther.* **15**, 1126–1130.
- Kishimoto, T., Morihara, Y., Osanai, M., Ogata, S., Kamitakahara, M., Ohtsuki, C. & Tanihara, M. 2005. Synthesis of poly(Pro-Hyp-Gly)(*n*) by direct poly-condensation of (Pro-Hyp-Gly)(*n*), where *n* = 1, 5, and 10, and stability of the triple-helical structure. *Biopolymers* **79**, 163–172.
- Lee, H., Sodek, K. L., Hwang, Q., Brown, T. J., Ringuette, M. & Sodek, J. 2007. Phagocytosis of collagen by fibroblasts and invasive cancer cells is mediated by MT1-MMP. *Biochem. Soc. Trans.* **35**, 704–706.
- Minakuchi, Y., Takeshita, F., Kosaka, N., Sasaki, H., Yamamoto, Y., Kouno, M., Honma, K., Nagahara, S., Hanai, K., Sano, A., Kato, T., Terada, M. & Ochiya, T. 2004. Atelocollagen-mediated synthetic small interfering RNA delivery for effective gene silencing *in vitro* and *in vivo*. *Nucleic Acids Res.* **32**, e109.
- Ochiya, T., Nagahara, S., Sano, A., Itoh, H. & Terada, M. 2001. Biomaterials for gene delivery: atelocollagen-mediated controlled release of molecular medicines. *Curr. Gene Ther.* **1**, 31–52.
- Stenzel, K. H., Miyata, T. & Rubin, A. L. 1974. Collagen as a Biomaterial. *Annu. Rev. Biophys. Bioeng.* **3**, 231–253.
- Tiemann, K. & Rossi, J. J. 2009. RNAi-based therapeutics-current status, challenges and prospects. *EMBO Mol. Med.* **1**, 142–151.
- Vooijs, M., Jonkers, J., Lyons, S. & Berns, A. 2002. Noninvasive imaging of spontaneous retinoblastoma pathway-dependent tumors in mice. *Cancer Res.* **62**, 1862–1867.

Original Article

Atelocollagen-mediated systemic administration of myostatin-targeting siRNA improves muscular atrophy in caveolin-3-deficient mice

Emi Kawakami,^{1†} Nao Kinouchi,^{1†} Taro Adachi,² Yutaka Ohsawa,³
Naozumi Ishimaru,⁴ Hideyo Ohuchi,² Yoshihide Sunada,³ Yoshio Hayashi,⁴
Eiji Tanaka¹ and Sumihare Noji^{2*}

¹Department of Orthodontics and Dentofacial Orthopedics, Institute of Health Bioscience, The University of Tokushima Graduate School, 3-18-15 Kuramoto, Tokushima 770-8504; ²Department of Life Systems, Institute of Technology and Science, The University of Tokushima, 2-1 Minami-Jyosanjima-cho, Tokushima 770-8506; ³Department of Neurology, Kawasaki Medical School, 577 Matsushima, Kurashiki City, Okayama 701-0192; and ⁴Department of Oral Molecular Pathology, Institute of Health Bioscience, The University of Tokushima Graduate School, 3-18-15 Kuramoto, Tokushima 770-8504, Japan

Small interfering RNA (siRNA)-mediated silencing of gene expression is rapidly becoming a powerful tool for molecular therapy. However, the rapid degradation of siRNAs and their limited duration of activity require efficient delivery methods. Atelocollagen (ATCOL)-mediated administration of siRNAs is a promising approach to disease treatment, including muscular atrophy. Herein, we report that ATCOL-mediated systemic administration of a myostatin-targeting siRNA into a caveolin-3-deficient mouse model of limb-girdle muscular dystrophy 1C (LGMD1C) induced a marked increase in muscle mass and a significant recovery of contractile force. These results provide evidence that ATCOL-mediated systemic administration of siRNAs may be a powerful therapeutic tool for disease treatment, including muscular atrophy.

Key words: atelocollagen, muscle, muscular dystrophy, myostatin, RNA interference.

Introduction

Myostatin (growth differentiation factor 8, GDF8) is a member of the transforming growth factor- β (TGF- β) superfamily of secreted growth factors (McPherron *et al.* 1997). A number of growth factors of this family have been shown to regulate cell growth and differentiation during development. Myostatin is unique among the members of the TGF- β superfamily because its expression is almost exclusively restricted to the skeletal muscle lineage.

Zhu *et al.* (2000) generated transgenic mice that expressed myostatin mutated at its cleavage site under the control of a muscle specific promoter creating a dominant negative myostatin. These mice exhibited a

significant (20–35%) increase in muscle mass that resulted from myofiber hypertrophy and not from myofiber hyperplasia. While, mice fully null for myostatin showed muscle masses that were nearly double that of normal muscle and this marked increase in muscle mass was associated with both hypertrophy and hyperplasia (McPherron *et al.* 1997). The difference in muscle mass seen in dominant negative myostatin and null myostatin mice likely results from incomplete dominance of dominant negative myostatin, so that dimerization and cleavage of normal myostatin is not fully blocked in dominant negative myostatin mice. So, lower levels of myostatin inhibition may affect hypertrophy, while higher levels of myostatin inhibition may be required to alter hyperplasia (Zhu *et al.* 2000). Thus, it appears that myostatin specifically downregulates skeletal muscle mass.

Because of its inhibitory role, myostatin downregulation may serve as a potentially important mechanism for treating diseases associated with muscle wasting and degeneration, such as muscular dystrophy. We recently demonstrated that myostatin inhibition induced by overexpression of the myostatin pro-domain prevented

*Author to whom all correspondence should be addressed.

Email: noji@bio.tokushima-u.ac.jp

[†]These authors contributed equally to this work.

Received 6 August 2010; revised 4 October 2010; accepted 4 October 2010.

© 2011 The Authors

Journal compilation © 2011 Japanese Society of Developmental Biologists

muscular atrophy and normalized intracellular myostatin signaling in a mouse model of limb-girdle muscular dystrophy 1C (LGMD1C) (Nishi *et al.* 2002). Furthermore, myostatin inhibition also suppressed muscular atrophy in caveolin-3-deficient mice that expressed a dominant-negative form of the caveolin-3 gene (Ohsawa *et al.* 2006). The dominant negative caveolin-3 mutation was a missense mutation (Pro104Leu) that was expressed under the control of the M-creatine kinase promoter (Sunada *et al.* 2001).

Duchenne muscular dystrophy (DMD) is an X-linked, lethal skeletal muscle disorder caused by mutations in the *dystrophin* gene (Bulfield *et al.* 1984; Yoshimura *et al.* 2007); it is a severe muscle wasting disorder that affects 1/3500 male births (Deconinck & Dan 2007). To date, there is no effective treatment for muscular dystrophy, although gene therapy could be a valuable approach to treating this disease. In a previous study, inhibition of myostatin using anti-myostatin blocking antibodies was employed in an effort to increase muscle mass (Bogdanovich *et al.* 2002). However, the generation of antibodies against recombinant target proteins was a time-consuming, labor-intensive approach.

Recently, RNA interference (RNAi) has emerged as an effective gene silencing method. RNAi refers to sequence-specific, post-transcriptional gene silencing mediated by approximately 22-nucleotide-long small interfering RNAs (siRNAs) generated from longer double-stranded RNAs (dsRNAs) in both plants and animals, ranging from flatworms to humans (Fire *et al.* 1998). RNAi-based approaches have increasingly been developed in which highly specific siRNAs designed to target disease-causing or disease-promoting genes are utilized without the induction of interferon synthesis or non-specific gene suppression (Elbashir *et al.* 2001; de Fougères *et al.* 2007). Magee *et al.* (2006) demonstrated that downregulation of myostatin expression via electroporation of a plasmid directing the expression of a short hairpin interfering RNA (shRNA) against myostatin led to a localized increase in skeletal muscle mass. For safety reasons, however, strategies using vector-based delivery systems may be of limited clinical use. Therefore, a more desirable approach would involve the direct application of active siRNAs *in vivo*.

Atelocollagen (ATCOL), a pepsin-treated type I collagen that lacks antigenicity-conferring telopeptides at its N and C termini, has been shown to promote the efficient delivery of chemically unmodified siRNAs to metastatic tumors *in vivo* (Minakuchi *et al.* 2004; Takeshita *et al.* 2005; Takeshita & Ochiya 2006). Based on its practical use as an siRNA delivery platform, we adapted an ATCOL-mediated oligonucleotide system to deliver a myostatin-targeting siRNA into muscle, and found that local or systemic administration of the

myostatin-targeting siRNA coupled with ATCOL led to a marked stimulation of muscle growth *in vivo* within a few weeks (Kinouchi *et al.* 2008). In the current study, we examined whether systemic administration of the myostatin-siRNA/ATCOL (Mst-siRNA/ATCOL) complex effectively silenced myostatin expression in LGMD1C mice, and whether it led to increased muscle mass and/or decreased muscle weakness. In the current study, we used the same myostatin-targeting siRNA reported previously (Magee *et al.* 2006), which is predicted to target myostatin mRNA not only in mice, but also in humans, rats, cows, macaques, and baboons.

Materials and methods

Systemic administration of the Mst-siRNA/ATCOL complex to skeletal muscles in LGMD1C mice

The Mst-siRNA and ATCOL complexes were prepared as follows. Equal volumes of siRNA solution (siRNA and 1x siRNA buffer, 40 $\mu\text{mol/L}$ final concentration) and ATCOL (0.05% final concentration) were combined and mixed by vigorous pipetting. For systemic administration, the siRNA/ATCOL complex (200 μL) was introduced intravenously via orbital veins into 20-week-old LGMD1C mice at 0, 4, 7 and 14 days. As a negative control, scrambled siRNAs were injected into 20-week-old LGMD1C mice at 0, 4, 7 and 14 days.

Morphometric analyses

The masseter and quadriceps femoris muscle tissues were dissected 3 weeks after the first Mst-siRNA/ATCOL complex administration. The tissues were snap-frozen in liquid nitrogen-cooled isopentane and sectioned transversely (6 μm) at the center of the masseter and quadriceps femoris muscles using a cryostat (Leica Microsystems). Sections were stained with hematoxylin and eosin (H&E), and fiber sizes were determined by measuring the area of each transversal myofiber within a fixed area. Approximately 100 myofibers were measured for each tissue sample (six to eight fields/tissue section).

Contractile properties of Mst-siRNA/ATCOL complex-treated tibialis anterior (TA) muscles

The entire tibialis anterior (TA) muscle was removed with its tibial origin intact, and the distal portion of the TA tendon, together with its origin, were secured with a 5-0 silk suture. The TA was then mounted in a vertical tissue chamber and connected to a force transducer, UL-10GR (Minerva, Nagano, Japan), and a length servosystem, MM-3 (Narishige, Tokyo, Japan).

Electrical stimulations were applied using a SEN3301 (Nihon Kohden, Tokyo, Japan) through a pair of platinum wires placed on both sides of the muscle in physiological salt solution (150 mmol/L NaCl, 4 mmol/L KCl, 2 mmol/L CaCl₂, 1 mmol/L MgCl₂, 5.6 mmol/L glucose, 5 mmol/L Hepes, pH 7.4, and 0.02 mmol/L D-tubocurarine). Muscle fiber length was adjusted incrementally using a micropositioner until peak isometric twitch force responses were obtained (optimal fiber length [L_0]). Maximal tetanic force (P_0) was assessed by stimulation frequencies of 125 pulses/s delivered in 500 ms duration trains with 2 min intervals between each train. After two measurements were taken, the stimulated muscles were weighted after the tendon and bone attachments were removed. All forces were normalized to the physiological cross-sectional area (pCSA), the latter estimated on the basis of the following formula: muscle wet weight (in mg)/(L_0 [in mm] × 1.06 [in mg/mm³]). The estimated pCSA was used to determine specific tetanic force, and the muscle was quickly frozen in liquid nitrogen-cooled isopentane for morphometric analysis.

Statistical analyses

Error bars indicate standard deviation of the mean. * indicates $P < 0.01$ or $P < 0.05$ in a Student's *t* test.

Results

The Mst-siRNA/ATCOL complex can stabilize and produce a long-term gene silencing effect

In initial experiments to evaluate the persistence and spread of siRNA/ATCOL complexes (100 μ L), we injected a BLOCK-iT Alexa Fluor Red Fluorescent Oligo (10 μ mol/L) in the masseter muscle of 20-week-old C57BL/6 mice. Mice were killed at 2 weeks, tissue samples were dissected, and Alexa Fluor Red Fluorescent Oligo expression was assessed under conditions identical to those used in myostatin gene transfer experiments. As expected, Alexa Fluor Red Fluorescent Oligo expression was detected near the sites of injection with an uneven distribution pattern across the tissue (Fig. 1, right panel). These observations suggested that the ATCOL and siRNA formed a stable complex capable of producing an efficient, long-term gene silencing effect.

Intravenous administration of myostatin-targeting siRNAs with ATCOL specifically repressed muscle atrophy in LGMD1C mice

Based on our observation that ATCOL formed stable complexes with siRNAs capable of long-term gene

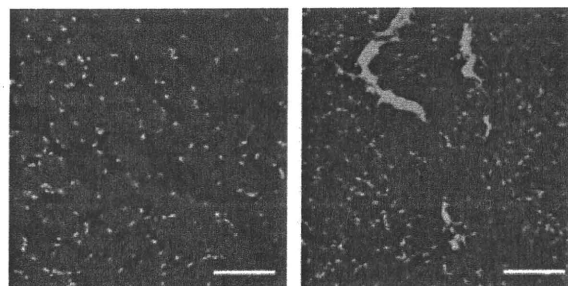


Fig. 1. Persistence and spread of an siRNA/atelocollagen (ATCOL, AteloGene Koken, Tokyo) complex following injection into the masseter muscle. A BLOCK-iT Alexa Fluor Red Fluorescent Oligo (10 μ mol/L final concentration, Invitrogen) and ATCOL (100 μ L) complex was injected into the masseter muscle of 20-week-old C57BL/6 mice. Gene expression from the BLOCK-iT Alexa Fluor Red Fluorescent Oligo/ATCOL complex injected in masseter muscle was assessed 2 weeks post-injection. Sections were examined following hematoxylin and eosin (H&E) staining (left) and serial section immunofluorescence to detect Alexa Fluor Red-positive cells (right). As expected, the Alexa Fluor Red Fluorescent Oligo expression was not evenly distributed across the tissue, and the majority of expression was located near the injection sites. Images were captured at 400 \times magnification. Scale bar, 100 μ m.

silencing, we administered Mst-siRNA/ATCOL or control scrambled siRNA/ATCOL complexes intravenously into 20-week-old LGMD1C mice at 0, 4, 7, and 14 days (Fig. 2A). Strikingly, we observed the enlargement of a number of skeletal muscles, including the lower limbs, masseters, and more in mice treated with Mst-siRNA/ATCOL (Fig. 2B). Since the changes in the lower limb muscles were the most pronounced, we used them for further analyses. Indeed, we also observed a significant increase in muscle fiber size at 3 weeks after the first administration in mice treated with Mst-siRNA/ATCOL (Fig. 2C).

These results indicated that intravenous administration of a myostatin-targeting siRNA with ATCOL specifically induced muscle hypertrophy in LGMD1C mice. The results were expressed as a ratio of the internal control and were analyzed statistically. Mst-siRNA/ATCOL-treated muscles ($18.64 \pm 4.18 \mu\text{m}$) were significantly larger than control muscles ($15.49 \pm 3.12 \mu\text{m}$) ($P < 0.0001$, $n = 100$). Histometric analysis showed that the myofibril sizes of quadriceps muscles treated with the Mst-siRNA/ATCOL complex were significantly larger than those of control quadriceps muscles (Fig. 2C,D). Examination of the sizes of 100 myofibers from each group showed that the Mst-siRNA/ATCOL-treated myofibril population exhibited a shift from smaller to larger sized fibers; the average myofibril size for Mst-siRNA/ATCOL-treated muscle was increased

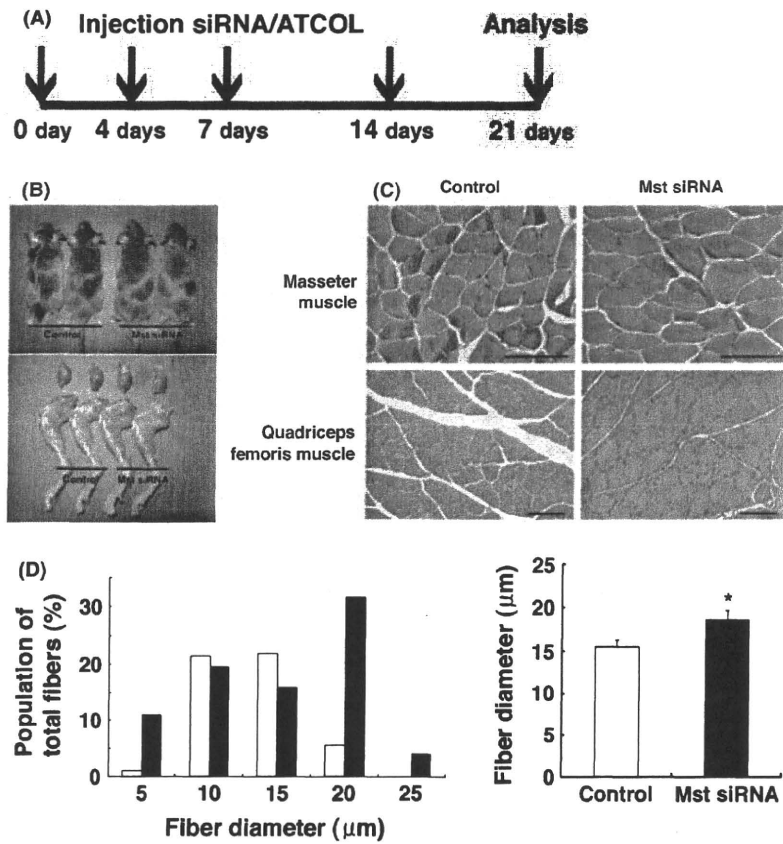


Fig. 2. Systemic administration of the Mst-siRNA/ATCOL complex led to increased skeletal muscle mass and fiber size in LGMD1C mice via inhibition of myostatin expression. In the experiments depicted in (A–C), Mst-siRNA (40 μmol/L final concentration) was mixed with ATCOL according to the manufacturer's instructions. (A) Time course analysis. Twenty-week-old male or female LGMD1C mice were anesthetized with Nembutal (25 mg/kg i.p.), and the Mst-siRNA/ATCOL complex (40 μmol/L in a 200 μL volume) was introduced intravenously via orbital veins at 0, 4, 7, and 14 days ($n = 3$). As a negative control, scrambled siRNAs were injected into LGMD1C mice. At 3 weeks after the first administration, the quadriceps muscles on both sides were harvested and processed for analysis. (B) Photographs of mice (upper panels) and lower limbs (lower panels). An increase in muscle mass was observed in the Mst-siRNA/ATCOL-treated (right), but not in control mice (left). (C) H&E staining of control (left) and Mst-siRNA/ATCOL-treated (right) masseter or quadriceps femoris muscle. Images of the masseter and quadriceps femoris were captured at 400x and 200x, respectively. Scale bar, 50 μm. (D) Distribution of the myofibril sizes of control (white bars) and Mst-siRNA/ATCOL-treated (black bars) quadriceps muscles. The right panel shows the average myofibril size (15.49 ± 3.12 μm vs. 18.64 ± 4.18 μm, respectively; $n = 100$; $P < 0.01$). The graphical representation of the data uses the following convention: mean ± SD. Mst-siRNA/ATCOL-treated muscles and mice are shown in black; control muscles and mice are shown in white. National Institute of Health (NIH) Image (NIH) software was used for morphometric measurements.

by approximately 1.2-fold relative to control muscle (Fig. 2D).

Hypertrophied Mst-siRNA/ATCOL-treated LGMD1C muscle fibers exhibit significantly improved contractile force generation

First, we tested the grip strength of mice before and after treatment. There were no statistically significant differences in the grip strength before and after treatment (Fig. 3D). We also evaluated the contractile properties of

Mst-siRNA/ATCOL-treated LGMD1C muscle (Fig. 3C). We did not identify any statistically significant differences in the wet weights of Mst-siRNA/ATCOL-treated and untreated LGMD1C muscle. Unexpectedly, the specific force of untreated LGMD1C muscle was much lower than that of Mst-siRNA/ATCOL-treated LGMD1C muscle (Fig. 3A,B). We analyzed the specific force generated by tetanic stimulation (150 Hz) of TA muscles from LGMD1C mice treated with ATCOL-based control scrambled siRNAs or Mst-siRNA (0.568 ± 0.293 vs. 0.041 ± 0.351 N/cm², respectively; $n = 4$; $P < 0.05$).

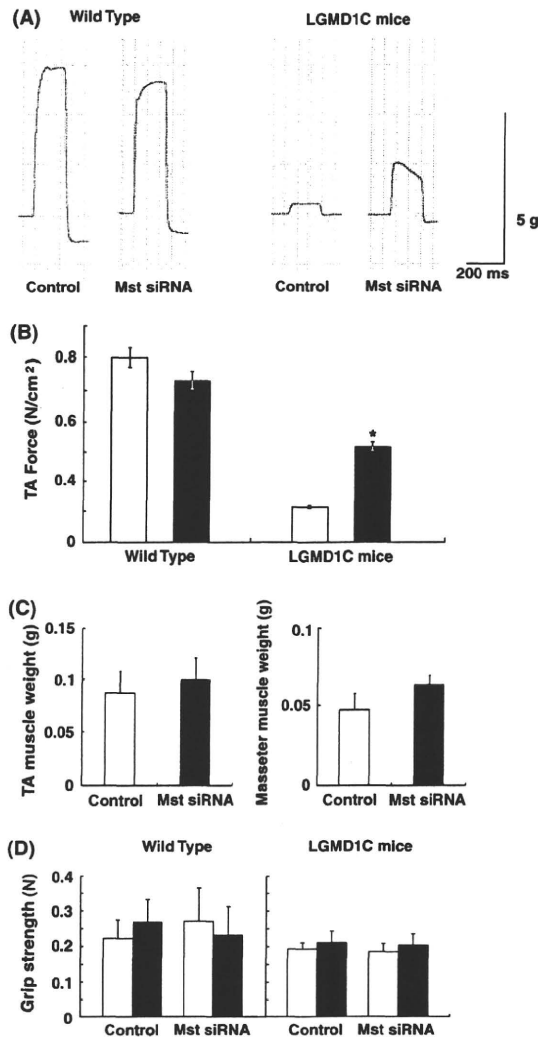


Fig. 3. Mst-siRNA/ATCOL-treated fibers exhibited significantly improved contractile force generation. (A) Specific force generated by tetanic stimulation (150 Hz) of TA muscles from wild-type or LGMD1C mice treated with ATCOL-based control scrambled siRNAs or Mst-siRNA. (B) The specific force of untreated LGMD1C muscle (□) was much lower than that of Mst-siRNA/ATCOL-treated LGMD1C muscle (■) (0.569 ± 0.293 N/cm² vs. 0.041 ± 0.351 N/cm², respectively; $n = 4$; $P < 0.05$). In contrast, in wild-type mice, the specific force was not different between untreated muscle and Mst-siRNA/ATCOL-treated muscle (0.888 ± 0.588 N/cm² vs. 0.925 ± 0.828 N/cm²; $n = 3$). (C) There were no statistically significant differences in wet weights between untreated muscles and Mst-siRNA/ATCOL-treated muscles. (D) There were no statistically significant differences in grip strength between pre-treated mice (□) and after Mst-siRNA/ATCOL-treated mice (■).

Although wild-type fibers have been found to be hypertrophied (Kinouchi *et al.* 2008), the present results did not show a significant difference between the contractile

force generated by Mst-siRNA/ATCOL-treated and untreated wild-type muscle (0.888 ± 0.588 vs. 0.925 ± 0.828 N/cm²; $n = 3$). As shown in Figure 2D, histogram analysis demonstrated a shift to the right in the fiber distribution of Mst-siRNA/ATCOL-treated LGMD1C muscle relative to that of untreated LGMD1C muscle; larger caliber fibers were dominant, reflecting hypertrophy of Mst-siRNA/ATCOL-treated muscle fibers. Thus, hypertrophied Mst-siRNA/ATCOL-treated LGMD1C muscle fibers exhibited improved contractile force generation, but the increase in muscle weight did not correlate with increased force generation.

We previously reported that local and systemic administration of siRNA against myostatin coupled with ATCOL markedly stimulated muscle growth *in vivo* within a few weeks (Kinouchi *et al.* 2008), and that ATCOL-based gene therapy was associated with low immunogenicity. As expected, we did not observe any signs or symptoms suggestive of health problems during the experimental period of the current study.

Discussion

In the current study, we intravenously administered a myostatin-targeting siRNA with ATCOL and analyzed the relationship between the extent of Mst-siRNA/ATCOL expression and the recovery of contractile force in LGMD1C muscles. Histogram analysis further demonstrated that the myofibril size distribution of Mst-siRNA/ATCOL-treated LGMD1C muscle fibers was shifted from smaller to larger sized fibers relative to control muscle fibers. We found that treatment of LGMD1C mice with the Mst-siRNA/ATCOL complex led to a significant increase in skeletal muscle mass and enhanced contractile force, similar to that reported previously with a myostatin blockade of dystrophic muscle (Bogdanovich *et al.* 2002).

There was no statistically significant difference in muscle weight between control and Mst-siRNA/ATCOL-treated muscles. It appeared that muscle weight did not correlate with force generation. Thus, hypertrophied Mst-siRNA-positive LGMD1C fibers seemed to greatly improve contractile force generation. Notably, the level of contractile force was dramatically improved by approximately 60% in Mst-siRNA/ATCOL-treated wild-type muscles relative to control muscles. Although the underlying molecular mechanisms by which Mst-siRNA/ATCOL treatment leads to increased contractile force remain to be determined, the current results are encouraging in that the function of caveolin-3-deficient muscles might be greatly improved. These findings are significant because the recovery of absolute maximal force and specific tetanic force are barometers of amelioration (Yoshimura *et al.* 2007).

To our knowledge, the results of the current study are the first to quantitatively and qualitatively demonstrate that *in vivo* myostatin siRNA gene transfer may serve as an effective treatment for muscular dystrophy. The potential benefit of myostatin siRNA gene therapy lies in the treatment of skeletal muscle waste in conditions such as muscular dystrophies (Bogdanovich *et al.* 2002), cachexia and HIV infection in advance of new therapies (Gonzalez-Cadavid & Bhasin 2004; Frimel *et al.* 2005). Although myostatin siRNA gene therapy would not correct the underlying pathophysiology of these diseases, it would counterbalance the effects by stimulating myofiber growth. The ease of administration of the myostatin-siRNA/ATCOL complex combined with its muscle-growth effect makes it a clinically valuable method of fighting against muscle atrophy. However, a strategy for the clinical use of this gene transfer method for human DMD patients requires further testing. Differences between humans and mice, including muscle size, life span and biological properties, should be taken into consideration (Yoshimura *et al.* 2007). In tumor-bearing mice, it was reported that ATCOL distributed siRNAs against luciferase to normal liver, lung, spleen and kidney tissues, as well as to bone-metastatic lesions (Takeshita *et al.* 2005). ATCOL was also reported to display low-toxicity and low-immunogenicity when it is transplanted *in vivo* (Ochiya *et al.* 2001; Sano *et al.* 2003).

Taken together, the results of the present study demonstrate that administration of siRNAs with ATCOL may be a promising therapeutic tool not only for muscular diseases, but also for other genetic diseases. The results of the current study indicate that treatment with Mst-siRNA/ATCOL led to an increase in muscle mass and functional recovery in the absence of obvious adverse effects in LGMD1C mice. The current study also provides evidence of ATCOL-mediated delivery of siRNA to skeletal muscle. Therefore, ATCOL-mediated administration of siRNAs represents a powerful new tool for future therapeutic use in the treatment of diseases, including muscular atrophy.

Acknowledgments

We thank Nami Naoe, Masahiro Fujino and Tadashi Okada (Division of Neurology, Kawasaki Medical School) for expert technical assistance. This work was supported by an intramural research grant (20B-13) for neurological and psychiatric disorders of NCNP and a research grant (H20-018) for comprehensive research on disability, health and welfare from the Ministry of Health, Labour and Welfare, a Grant for Research on Psychiatric and Neurological Diseases and Mental Health from the Ministry of Health, Labour and Welfare

of Japan (15131301) to Y.O, funding from JSPS KAKENHI (14370212) to YS and Research Project Grants from Kawasaki Medical School (15-115B and 16-601) to Y.O. and Y.S.

References

- Bogdanovich, S., Krag, T. O., Barton, E. R., Morris, L. D., Whittemore, L. A., Ahima, R. S. & Khurana, T. S. 2002. Functional improvement of dystrophic muscle by myostatin blockade. *Nature* **420**, 418–421.
- Bulfield, G., Siller, W. G., Wight, P. A. & Moore, K. J. 1984. X chromosome-linked muscular dystrophy (mdx) in the mouse. *Proc. Natl Acad. Sci. USA* **81**, 1189–1192.
- Deconinck, N. & Dan, B. 2007. Pathophysiology of duchenne muscular dystrophy: current hypotheses. *Pediatr. Neurol.* **36**, 1–7.
- de Fougères, A., Vornlocher, H. P., Maraganore, J. & Lieberman, J. 2007. Interfering with disease: a progress report on siRNA-based therapeutics. *Nat. Rev. Drug. Discov.* **6**, 443–453.
- Elbashir, S. M., Harborth, J., Lendeckel, W., Yalcin, A., Weber, K. & Tuschl, T. 2001. Duplexes of 21-nucleotide RNAs mediate RNA interference in cultured mammalian cells. *Nature* **411**, 494–498.
- Fire, A., Xu, S., Montgomery, M. K., Kostas, S. A., Driver, S. E. & Mello, C. C. 1998. Potent and specific genetic interference by double-stranded RNA in *Caenorhabditis elegans*. *Nature* **391**, 806–811.
- Frimel, T. N., Kapadia, F., Gaidosh, G. S., Li, Y., Walter, G. A. & Vandenberg, K. 2005. A model of muscle atrophy using cast immobilization in mice. *Muscle Nerve* **32**, 672–674.
- Gonzalez-Cadavid, N. F. & Bhasin, S. 2004. Role of myostatin in metabolism. *Curr. Opin. Clin. Nutr. Metab. Care* **7**, 451–457.
- Kinouchi, N., Ohsawa, Y., Ishimaru, N., Ohuchi, H., Sunada, Y., Hayashi, Y., Tanimoto, Y., Moriyama, K. & Noji, S. 2008. Atelocollagen-mediated local and systemic administrations of myostatin-targeting siRNA increase skeletal muscle mass. *Gene Ther.* **15**, 1126–1130.
- Magee, T. R., Artaza, J. N., Ferrini, M. G., Vernet, D., Zuniga, F. I., Cantini, L., Reisz-Porszasz, S., Rajfer, J. & Gonzalez-Cadavid, N. F. 2006. Myostatin short interfering hairpin RNA gene transfer increases skeletal muscle mass. *J. Gene Med.* **8**, 1171–1181.
- McPherron, A. C., Lawler, A. M. & Lee, S. J. 1997. Regulation of skeletal muscle mass in mice by a new TGF- β superfamily member. *Nature* **387**, 83–90.
- Minakuchi, Y., Takeshita, F., Kosaka, N., Sasaki, H., Yamamoto, Y., Kouno, M., Honma, K., Nagahara, S., Hanai, K., Sano, A., Kato, T., Terada, M. & Ochiya, T. 2004. Atelocollagen-mediated synthetic small interfering RNA delivery for effective gene silencing in vitro and in vivo. *Nucleic Acids Res.* **32**, e109.
- Nishi, M., Yasue, A., Nishimatu, S., Nohno, T., Yamaoka, T., Itakura, M., Moriyama, K., Ohuchi, H. & Noji, S. 2002. A missense mutant myostatin causes hyperplasia without hypertrophy in the mouse muscle. *Biochem. Biophys. Res. Commun.* **293**, 247–251.
- Ochiya, T., Nagahara, S., Sano, A., Itoh, H. & Terada, M. 2001. Biomaterials for gene delivery: atelocollagen-mediated controlled release of molecular medicines. *Curr. Gene Ther.* **1**, 31–52.
- Ohsawa, Y., Hagiwara, H., Nakatani, M., Yasue, A., Moriyama, K., Murakami, T., Tsuchida, K., Noji, S. & Sunada, Y. 2006.

- Muscular atrophy of caveolin-3-deficient mice is rescued by myostatin inhibition. *J. Clin. Invest.* **116**, 2924–2934.
- Sano, A., Maeda, M., Nagahara, S., Ochiya, T., Honma, K., Itoh, H., Miyata, T. & Fujioka, K. 2003. Atelocollagen for protein and gene delivery. *Adv. Drug Deliv. Rev.* **55**, 1651–1677.
- Sunada, Y., Ohi, H., Hase, A., Ohi, H., Hosono, T., Arata, S., Higuchi, S., Matsumura, K. & Shimizu, T. 2001. Transgenic mice expressing mutant caveolin-3 show severe myopathy associated with increased nNOS activity. *Hum. Mol. Genet.* **10**, 173–178.
- Takeshita, F., Minakuchi, Y., Nagahara, S., Honma, K., Sasaki, H., Hirai, K., Teratani, T., Namatame, N., Yamamoto, Y., Hanai, K., Kato, T., Sano, A. & Ochiya, T. 2005. Efficient delivery of small interfering RNA to bone-metastatic tumors by using atelocollagen in vivo. *Proc. Natl Acad. Sci. USA* **102**, 12177–12182.
- Takeshita, F. & Ochiya, T. 2006. Therapeutic potential of RNA interference against cancer. *Cancer Sci.* **97**, 689–696.
- Yoshimura, M., Sakamoto, M., Ikemoto, M., Mochizuki, Y., Yuasa, K., Miyagoe-Suzuki, Y. & Takeda, S. 2007. AAV vector-mediated microdystrophin expression in a relatively small percentage of mdx myofibers improved the mdx phenotype. *Mol. Ther.* **15**, 320–329.
- Zhu, X., Hadhazy, M., Wehling, M., Tidball, J. G. & McNally, E. M. 2000. Dominant Negative myostatin produces hypertrophy without hyperplasia in muscle. *FEBS Lett.* **474**, 71–75.

RNA干渉法による治療を実現するための研究

野地 澄晴 徳島大学大学院ソシオテクノサイエンス研究部
 足立 太郎 徳島大学大学院先端技術科学教育部
 川上 恵実 徳島大学大学院歯学研究科
 田中 栄二 徳島大学大学院ヘルスバイオサイエンス研究部

要旨

RNA干渉 (RNA interference (RNAi)) は、細胞内で二本鎖RNAと相補的な塩基配列を持つmRNAが分解される現象である。この現象を利用して人工的に二本鎖RNAを導入することにより、任意の遺伝子の発現を抑制することができるため、疾患原因遺伝子などの発現を標的とした治療にRNA干渉法が使用できると考えられている。しかし、この治療法を実現するには2つの大きな課題が残っている。1つは、small interfering RNA (siRNA) のデリバリー法の問題で、標的の細胞にどのようにして生体内で不安定なsiRNAを導入するかであり、2つ目はsiRNAを合成するコストが高価であることである。われわれは最初の課題に取り組み、コラーゲンを利用したsiRNAのデリバリー法について検討してきた。特に、慢性筋萎縮疾患である筋ジストロフィーなどの治療を例として、筋ジストロフィーモデル雄性マウス咬筋に対して骨格筋形成抑制遺伝子マイオスタチンのsiRNAとアテロコラーゲンあるいは合成コラーゲンの複合体を局所投与し、咬筋におけるRNA干渉効果を検討してきた。また全身投与することによって咬筋だけでなく、前頸部筋でのRNA干渉効果を検討し、機能的解析を行ってきた。臨床応用を考慮に入れ、siRNAとアテロコラーゲンおよび特殊加工コラーゲン複合体の研究についての研究成果について紹介する。

1. 序 論

1998年にFireらは線虫の一種である*Caenorhabditis elegans* (*C.elegans*) を用いて、RNA干渉 (RNA interference (RNAi)) という現象を発見した⁽¹⁾。この現象は、その後、ヒトに至るまで多くの生物が共通に持つ現象であることがわかった⁽²⁾。特に、siRNA (small interfering RNA) と呼ばれる21-23個の塩基からなる短い3' 突出型二本鎖RNAがその主役であり、siRNAがいくつかの蛋白質複合体に結合し、相補的な配列を持つmRNAを分解することがわかった⁽³⁾。2001年には哺乳類の細胞でsiRNAを導入することで、それまで問題となってきた二本鎖RNA依存性の免疫応答反応を回避することができることがわかった。これにより、遺伝子異常が原因の疾患に対するRNA干渉治療が可能であると考えられ、応用への期待が高まってきた。2006年には、アンドリュー・ファイアーとクレイグ・メローはRNAi発見の功績によりノーベル生理学・医学賞を受賞した。

RNA干渉を利用した治療を考える場合に、2つの大きな壁が存在している。1つは、siRNAのデリバリーの問題で、2つ目は、siRNAの合成費用が高いことである。2つ目の問題については、核酸合成に関する画期的な方法が開発されるか、RNA合成酵素を利用した方法の開発が必要である。一方、最初の問題については、多くの研究者が研究しており、次々と新しい方法が提案

されている⁽⁴⁻⁸⁾。我々はRNA干渉のための新規なsiRNAのデリバリー法として、コラーゲンに着目して研究を行っている。

これまでの研究経過を簡単に紹介する。通常、遺伝子の機能阻害 (ノックアウト) 実験を行うためには、染色体上の遺伝子に突然変異を導入することで行われてきた。そのため、マウスなどの動物の遺伝子操作が必要であり、非常に時間のかかる実験である。しかし、RNA干渉法を用いた遺伝子の発現低下 (ノックダウン) 実験は、比較的簡単で、塩基配列さえ知ることができれば合成したsiRNAを導入することで結果を得ることができる。もちろん、ノックアウトとノックダウンでは得られる結果はまったく同じではないが、ゲノムプロジェクトによって全塩基配列を知ることのできる生物種では、遺伝子発現のノックダウンにより遺伝子の機能解析の速度を上げることが可能となる。さらに、ヒト疾患の治療を考えた場合、事実上ノックアウト法の使用は困難な治療であることから、ノックダウン法しか実質的には使用できないと考えられる。

森山啓司と野地澄晴のグループは、筋肉の形成を抑制する因子であるマイオスタチンの研究を行い、マイオスタチンの発現が抑制されたトランスジェニックマウスを用いて、筋肉が過剰に形成されることを示してきた⁽⁹⁾。また、マイオスタチンの発現抑制により、筋ジストロ

フィーのモデルトランスジェニックマウスにおいて、筋肉の機能が回復することを示してきた⁽¹⁰⁾。

そこで、現実的な治療方法と臨床応用のための研究として、マイオスタチンの発現抑制をRNA干渉法により行う方法について検討を行ってきた。このRNA干渉治療法では、マイオスタチンのmRNAの一部に相補的な21から25塩基配列を持つsiRNAを生体内に導入し、遺伝子の発現を抑制することを試みた。siRNAを非侵襲的かつ安全に臨床応用に用いる方法は、現在までに様々に開発されてきているが、我々は比較的処理が簡単な、アテロコラーゲン(ATCOL)(高研(株))を用いたsiRNA導入キットを用いてまず検討を行った。

次に臨床応用でのコスト面の問題点を改善する事を目的に、RNA干渉のための新規なsiRNAのデリバリー法としてATCOLの代替となり得る安価で安全性のある特殊加工コラーゲン(SYCOL)をsiRNAの導入試薬として使用してRNAi効果の検討を行った。

具体的には、1) マウス骨格筋にマイオスタチン遺伝子に対するsiRNA(*Mst*-siRNA)とATCOLの複合体を投与し、RNAi効果を検討した⁽¹¹⁾。2) SYCOLの開発を行い、*in vivo*, *in vitro*, siRNAのRNaseによる分解阻害でATCOLとSYCOLの比較検討を行った⁽¹²⁾。これらの研究について紹介する。

2. 研究方法について

- 1) (1) 24~28週齢の野生型(C57BL/6)雄性マウスの右側咬筋と大腿二頭筋に*Mst*-siRNAとATCOL複合体の局所投与を行い、2週間後に咬筋と大腿二頭筋を摘出し、その筋重量を測定するとともに、形態学的ならびに組織学的解析を実施した。なお、同一個体の左側咬筋および大腿二頭筋を対照側としてスクランブルsiRNA(*scr*-siRNA)とATCOL複合体を投与し、*Mst*-siRNA導入を行った実験側との比較を行った。若いマウスについては、*Mst*の産生が少なく、効果はほとんど観察されなかった。
- (2) 24~28週齢の野生型(C57BL/6)雄性マウスに*Mst*-siRNAとATCOL複合体の全身投与を2週間の間に4回を行い、最終投与から1週間の待機期間の後に大腿筋を摘出し、その筋重量を測定するとともに、形態学的ならびに組織学的解析を実施した。
- (3) 24~28週齢のDuchenne型筋ジストロフィーモデル動物である*mdx*マウスの雄を用いて右側咬筋に*Mst*-siRNAとATCOL複合体の局所投与を行い、2週間後に咬筋を摘出し、その筋重量を測定するとともに、形態学的ならびに組織学的解析を実施した。なお、同一個体の左側咬筋を対照側として*scr*-siRNAと

ATCOL複合体を投与し、比較した。

- 2) (1) siRNAと特殊加工コラーゲン(SYCOL)の複合体にRNaseを接触させ、siRNAが完全に分解するまでの時間を計測し、RNaseプロテクシオン能力をATCOLと比較、検討した。
- (2) ルシフェラーゼを恒常発現するB16-F10-luc-G5細胞にルシフェラーゼに対するsiRNA(*Luc*-siRNA)とSYCOLの複合体によってトランスフェクションを行い、RNAi効力による定量的なルシフェラーゼ発現量現象を測定した。
- (3) 1) (1)と同様に24~28週齢の野生型(C57BL/6)雄性マウスの右側咬筋に*Mst*-siRNAとSYCOLまたはATCOL複合体の局所投与を行い、2週間後に咬筋を摘出し、その筋重量を測定するとともに、形態学的ならびに組織学的解析を実施し、SYCOLとATCOLのRNAi効力を比較検討した。
- (4) ノードマウスを用い、右目眼窩底静脈からルシフェラーゼを恒常発現するガン細胞のB16-F10-luc-G5細胞を血流に流し全身転移させた。7日後、全身転移したB16-F10-luc-G5細胞のルシフェラーゼの発現を左目眼窩底静脈から*Luc*-siRNAとSYCOLまたはATCOLの複合体を全身投与することでSYCOLの全身投与でのRNAi効力を検討した。

3. RNA干渉法による筋肉治療のための基礎実験について

- 1) (1) マウス咬筋ならびに大腿二頭筋への*Mst*-siRNA/アテロコラーゲン複合体の局所投与と実験の結果は下記のように報告されている⁽¹¹⁾。
マウス咬筋の肉眼的所見では、*Mst*-siRNAを導入していない右側咬筋および大腿二頭筋(対照側)と比較して*Mst*-siRNAを導入した左側同部位では著明な骨格筋増大が認められた(Fig. 1 a)。また、その骨格筋の重量測定を行ったところ、*Mst*-siRNAを導入した咬筋および大腿二頭筋の骨格筋重量は対照側に比べ、いずれも有意に増加していた(Fig. 1 b)。組織学的検討を行うために上記同部位の骨格筋組織にて凍結切片を作成し、HE染色を行ったところ、対照群に比べ*Mst*-siRNAを導入した咬筋の最大直径部における筋線維は有意に肥大傾向を示した(Fig. 1 d, e)。また、咬筋におけるマイオスタチンの発現をウエスタンブロット法にて解析したところ、対照側と比較して*Mst*-siRNAを導入した咬筋では顕著なマイオスタチンの発現抑制が認められた(Fig. 1 c)。
- (2) マウスへの*Mst*-siRNA/アテロコラーゲン複合体の全身投与と実験については、下記のように

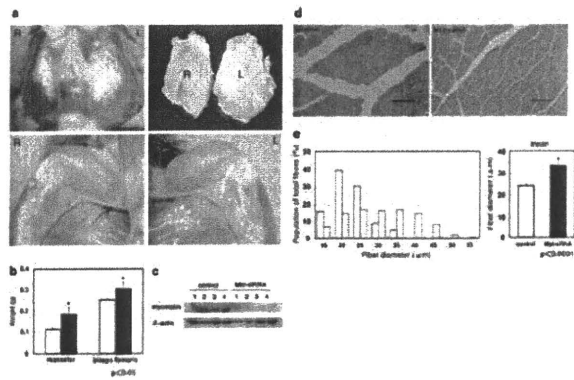


Fig. 1

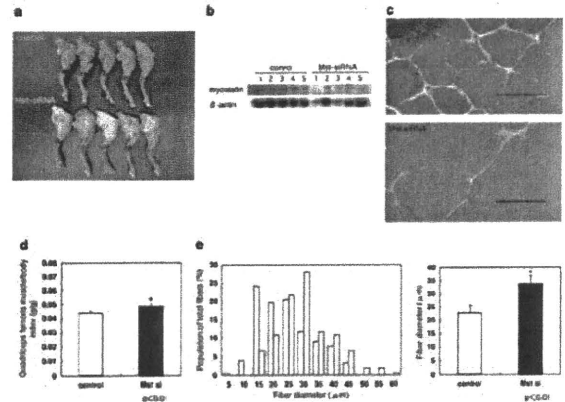


Fig. 2

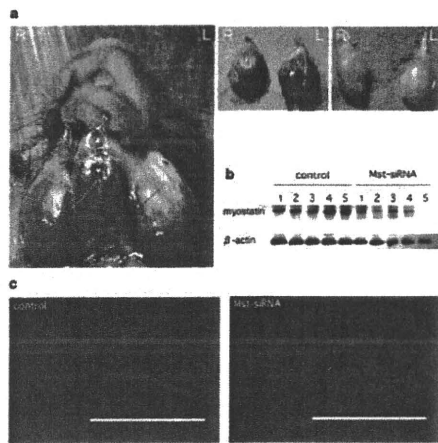


Fig. 3

報告されている⁽¹¹⁾。

マウス大腿二頭筋の肉眼所見では *Mst*-siRNA を導入していない対照群と比較して、*Mst*-siRNA を導入した実験群での著明な筋増大が見られた (Fig. 2 a), 筋重量についても *Mst*-siRNA 導入群で有意に増加していた (Fig. 2 d)。局所投与時と同様、組織学的検討のために HE 染色を行ったところ、対照群に比べ、*Mst*-siRNA を導入した咬筋の最大直径部における筋線維の太さを計測したところ、有意に肥大傾向を示した (Fig. 2 c, e)。大腿二頭筋におけるマイオスタチンの発現をウエスタンブロット法にて解析したところ、対照群と比較して *Mst*-siRNA を導入した実験群の大腿二頭筋では顕著なマイオスタチンの発現抑制が認められた (Fig. 2 b)。

(3) *mdx* マウス咬筋への *Mst*-siRNA/アテロコラーゲン複合体の局所投与実験の結果は、RNA 干渉治療の可能性を示唆するものであった⁽¹¹⁾。

マウス咬筋の肉眼所見では、*Mst*-siRNA を導入していない対照側と比較して、*Mst*-siRNA を導入した実験側での著明な筋増大が見られた

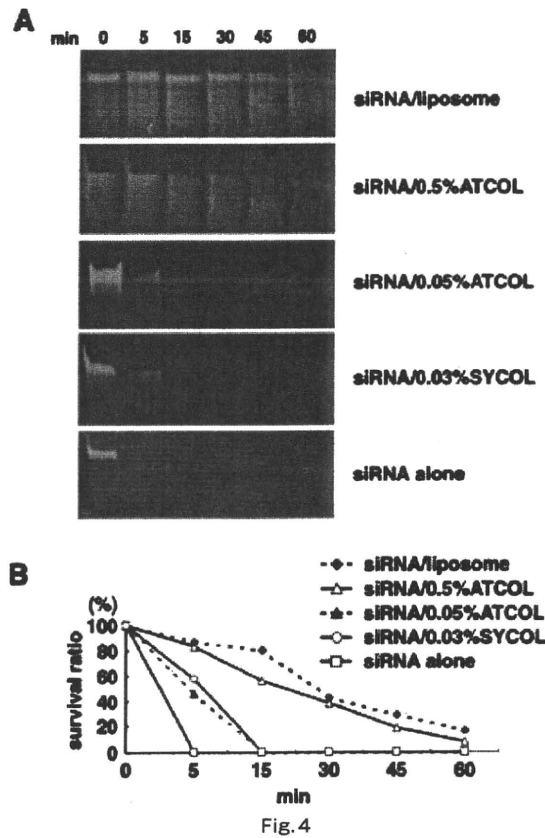


Fig. 4

(Fig. 3 a)。組織学的検討の為、凍結切片に対して抗ラミニン-*a* 抗体を用いた蛍光免疫染色を行ったところ、筋細胞壁が染色され、対照側と比較して *Mst*-siRNA 導入した実験側での筋繊維直径の増大が明らかとなった (Fig. 3 c)。また、咬筋におけるマイオスタチンの発現をウエスタンブロット法にて解析したところ、対照側と比較して *Mst*-siRNA を導入した咬筋では顕著なマイオスタチンの発現抑制が認められた (Fig. 3 b)。

2) (1) RNaseからのプロテクションアッセイの結果について⁽¹²⁾

siRNA/リポソーム, 0.5% ATCOL, 0.05% ATCOL, 0.03% SYCOL 複合体でRNaseからのプロテクションアッセイを行った結果, リポソームと0.5% ATCOLは同等の結果, 0.05% ATCOLは0.03% SYCOLと同等の結果となった。(Fig.4)

(2) in vitroでのsiRNA/SYCOLのトランスフェクション実験について⁽¹²⁾

siRNA/リポソーム, ATCOL, SYCOL 複合体でB16-F10-luc-G5細胞のルシフェラーゼをLuc-siRNAで抑制した結果, リポソーム, ATCOL, SYCOLともに同等のノックダウン結果となった。(Fig.5)

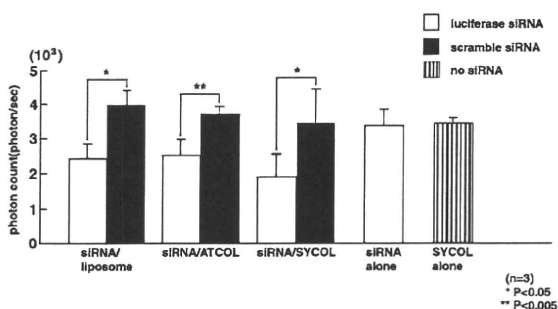


Fig.5

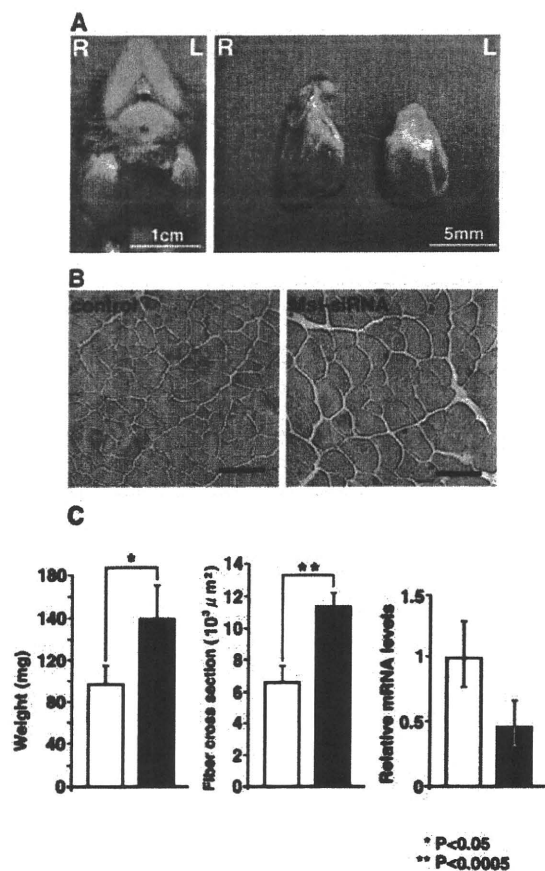


Fig.6

(3) in vivoでのsiRNA/SYCOL局所投与実験について⁽¹²⁾

SYCOLを用いてMst-siRNAをマウス咬筋に局所投与し, その影響を調べた結果, ATCOLと同様に一度投与しただけで, 2週間後には肉眼的に筋肉の増大を確認できた。Mst-siRNAとSYCOLの複合体投与の右側咬筋は, 対照側と比較して筋重量, 筋線維断面積ともに有意に増加し, mRNAの発現も有意に減少していた (Fig. 6)。また, SYCOLとATCOLのmRNAサイレンシング能は同等の結果となった (Fig.7)。

(4) in vivoでのsiRNA/SYCOL全身投与実験について⁽¹²⁾

全身でのsiRNA/SYCOLおよびATCOLのRNAi効力を検証するためにヌードマウスに全身転移させたルシフェラーゼ発現メラノーマ細胞をLuc-siRNAでノックダウンし, バイオイメージングIVISで撮影した結果 (Fig. 8 A), ATCOLは腹部のルシフェラーゼの発現も抑制したが (Fig. 8 B), SYCOLは投与した付近の発現のみを抑制していた (Fig. 8 C)。

4. RNA干渉法による筋肉治療は可能であろう

近年, 核酸医薬, 特にsiRNAのデリバリーシステムの開発が進められているが⁽⁴⁻⁸⁾, 血中あるいは組織中においてsiRNAの安定化は困難だと考えられてきた。今回の実験でコラーゲンを基材としたトランスフェクション試薬の咬筋および大腿二頭筋への局所投与, 全身投与は1週間を超える長期間でのRNAiの効力を発揮することが認められた。また, Duchenne型筋ジストロフィーモデルマウスのmdxマウスへのMst-siRNAの局所投与においては筋肉萎縮の回復が認められた。

また, 新規siRNAトランスフェクション試薬であるSYCOLはin vitro, in vivo局所投与でATCOLと同等の

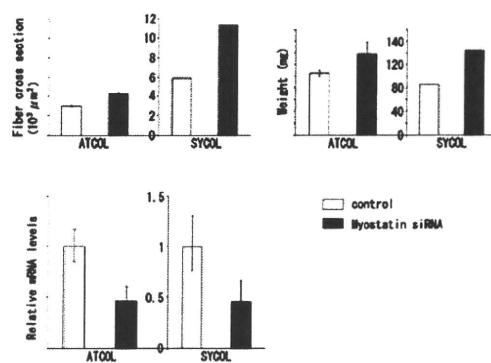


Fig.7

効力を確認することができた。しかしながらSYCOLの in vivo 全身投与に関してはこれからの課題である。今後このような技術が直接成体に対して応用できる新たな治療法として進歩し、非侵襲的かつ安全に行うことが可能となれば、骨格筋異常を伴う疾患を持つ患者だけでなく様々な疾患に対するRNAi創薬の可能性がますます広がるものと期待される。

5. 結論

ATCOLおよびSYCOLとMst-siRNA複合体の局所導入は、筋肉内に発現するマイオスタチン遺伝子を特異的に抑制し、咬筋形成に影響を及ぼすことが示された。また、ATCOLとMst-siRNA複合体の全身投与において大腿二頭筋の肥大を示したことから、骨格筋形成量の制御法として有効であることがわかった。また、臨床応用で筋肉以外の部位のガン細胞でATCOLおよびSYCOLとsiRNA複合体の効力を検討した結果、同様にRNAi効力があることが認められ、RNAi治療薬が幅広く疾患に

応用できる可能性が示唆された。

1. Fire, A., Xu, S., Montgomery, M. K., Kostas, S. A., Driver, S. E., and Mello, C. C. 1998. Potent and specific genetic interference by double-stranded RNA in *Caenorhabditis elegans*. *Nature* 391 : 806-811.
2. Bernstein, E., Caudy, A.A., Hammond, S.M., and Hannon, G.J. 2001. Role for a bidentate ribonuclease in the initiation step of RNA interference. *Nature* 409 : 363-366.
3. Elbashir, S.M., Harborth, J., Lendeckel, W., Yalcin, A., Weber, K., and Tuschl, T. 2001. Duplexes of 21-nucleotide RNAs mediate RNA interference in cultured mammalian cells. *Nature* 411 : 494-498.
4. Kim, S.S., Garg, H., Joshi, A., and Manjunath, N. 2009. Strategies for targeted nonviral delivery of siRNAs in vivo. *Trends Mol Med* 15 : 491-500.
5. Kim, W.J., and Kim, S.W. 2009. Efficient siRNA delivery with non-viral polymeric vehicles. *Pharm Res* 26 : 657-666.
6. Minakuchi, Y., Takeshita, F., Kosaka, N., Sasaki, H., Yamamoto, Y., Kouno, M., Honma, K., Nagahara, S., Hanai, K., Sano, A., et al. 2004. Atelocollagen-mediated synthetic small interfering RNA delivery for effective gene silencing in vitro and in vivo. *Nucleic Acids Res* 32 : e109.
7. Dykxhoorn, D.M., and Lieberman, J. 2006. Knocking down disease with siRNAs. *Cell* 126 : 231-235.
8. Xie, F.Y., Woodle, M.C., and Lu, P.Y. 2006. Harnessing in vivo siRNA delivery for drug discovery and therapeutic development. *Drug Discov Today* 11 : 67-73.
9. Nishi, M., Yasue, A., Nishimatu, S., Nohno, T., Yamaoka, T., Itakura, M., Moriyama, K., Ohuchi, H., and Noji, S. 2002. A missense mutant myostatin causes hyperplasia without hypertrophy in the mouse muscle. *Biochem Biophys Res Commun* 293 : 247-251.
10. Ohsawa, Y., Hagiwara, H., Nakatani, M., Yasue, A., Moriyama, K., Murakami, T., Tsuchida, K., Noji, S., and Sunada, Y. 2006. Muscular atrophy of caveolin-3-deficient mice is rescued by myostatin inhibition. *J Clin Invest* 116 : 2924-2934.
11. Kinouchi, N., Ohsawa, Y., Ishimaru, N., Ohuchi, H., Sunada, Y., Hayashi, Y., Tanimoto, Y., Moriyama, K., and Noji, S. 2008. Atelocollagen-mediated local and systemic applications of myostatin-targeting siRNA increase skeletal muscle mass. *Gene Ther* 15 : 1126-1130.
12. Adachi, T., Kawakami, E., Ishimaru, N., Ochiya, T., Hayashi, Y., Ohuchi, H., Tanihara, M., Tanaka, E., and Noji, S. 2010. Delivery of small interfering RNA with a synthetic collagen poly (Pro-Hyp-Gly) for gene silencing in vitro and in vivo. *Dev Growth Differ* 52 : 8.

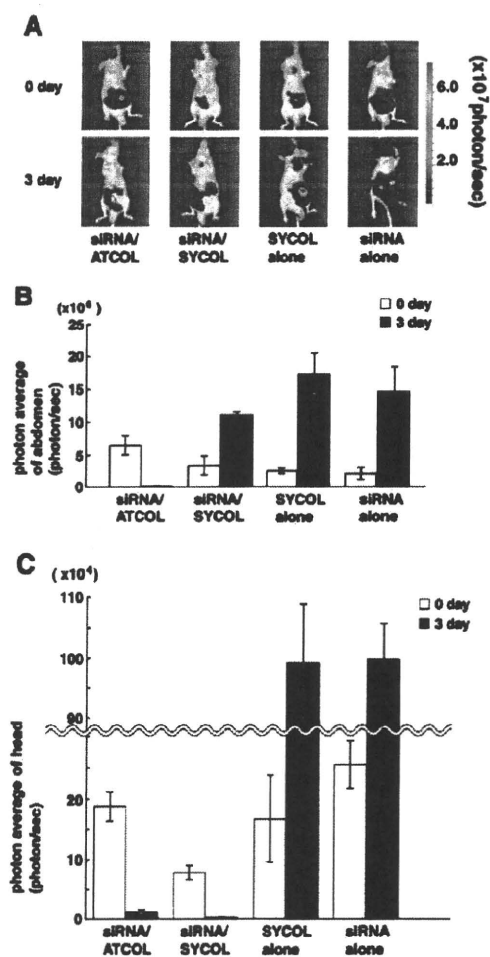


Fig. 8